富山大学研究推進機構水素同位体科学研究センター研究報告 37：29－38，2017.

ノート

種結晶法による CHA 型ゼオライトの繰り返し合成と構造変化

田口 明*，中森拓実，米山優紀

富山大学　研究推進機構　水素同位体科学研究センター

〒930-8555　富山市五福 3190

Synthesis and Structural Change of CHA Type Zeolite in the Repeated Seed-Growth Synthesis

Akira Taguchi*, Takumi Nakamaori, Yuki Yoneyama

Hydrogen Isotope Research Center

Organization for Promotion of Research, University of Toyama

Gofuku 3190, Toyama 930-8555

(Received January 19, 2018; accepted June 22, 2018)

Abstract

The synthesis of CHA type zeolite using seed crystals was studied. CHA zeolite could be obtained by seeded growth synthesis, where the initial seeds of CHA zeolite were prepared by the hydrothermal conversion of FAU zeolite. However, the subsequent use of the resultant CHA zeolite as seed crystals resulted in a structure change to sanidine and analcine.

Research note

Zeolites have applications in a variety of fields including detergent builders, adsorbents/desiccants and catalysts [1]. Recently, chabazite type zeolites, comprising 8-membered rings and assigned the framework type CHA by the International Zeolite Association [2], have been attracting new attention. This is because high silica CHA zeolite (so-called SSZ-13) or silicoaluminophosphate (SAPO-34) catalyzes the methanol-to-olefin reaction with high olefin (ethylene and propylene) selectivity [3-5]. More recent studies have shown that CHA zeolite, especially, copper-ion exchanged SSZ-13 (Cu-SSZ-13), provides a high NOx reduction activity using NH_3 as a reductant (NH_3-SCR) [6-8].

There are two main methods for the synthesis of CHA zeolite. One is a widely known, reliable method with potential applicability to the synthesis of SSZ-13, which uses N,N,N-trimethyladamantammonium hydroxide as an organic structure directing agent (OSDA) [5,9-11]. The other is the structure conversion method, where a well-defined zeolite is hydrothermally converted to CHA zeolite. Using FAU type zeolite as the starting material is probably the most popular method for CHA synthesis [12]. We also prepared CHA zeolite (K^+-type) from FAU (H-Y) zeolite, and found an intrinsic H_2 and D_2 sorption properties in subsequently Na^+ or Ca^{2+} ion-exchanged CHA zeolites [13].

One drawback of this CHA zeolite synthesis, especially for SSZ-13, is the use of expensive OSDA. This underscores the importance of developing CHA zeolite synthesis without requiring OSDA. Using seed crystals of CHA zeolite in zeolite growth is a progressive process, and Imai et al. successfully achieved seed-assisted CHA zeolite growth [14]. Also, Liu et al. reported the ultrafast (within 10 min) synthesis of CHA zeolite by using a continuous-flow reactor [15]. However, the initial seed crystals of CHA used in their experiments were prepared using OSDA. In the present report, we studied the seed-assisted growth of CHA zeolite, where the initial CHA zeolite was prepared by structure conversion method from FAU

zeolite.

Potassium type CHA zeolite was prepared by the hydrothermal conversion of FAU zeolite as described in the literature [9,10]. To 16.1 mL of a KOH (45 wt%) aqueous solution, 15 g of HY-zeolite (HSZ-320HOA, Tosoh Corp.) was added. Then, 119 mL of deionized water was poured, followed by vigorous shaking for 30 sec. The mixed solution was kept static in an oven at 100 ºC for 4 days. After cooling to room temperature, the precipitate was recovered by filtration, washed with water, and dried overnight at 100 ºC. The white solid was calcined at 600 ºC for 3 h under air flow (ca. 100 cm^3/min), with a ramp rate of 2 ºC/min. The obtained sample was denoted as CHA-HT. Figure 1 (a) shows the XRD (X-ray diffraction) patterns of CHA-HT. The diffraction signals were assignable to those from the CHA structure [2], suggesting the successful preparation of CHA zeolite.

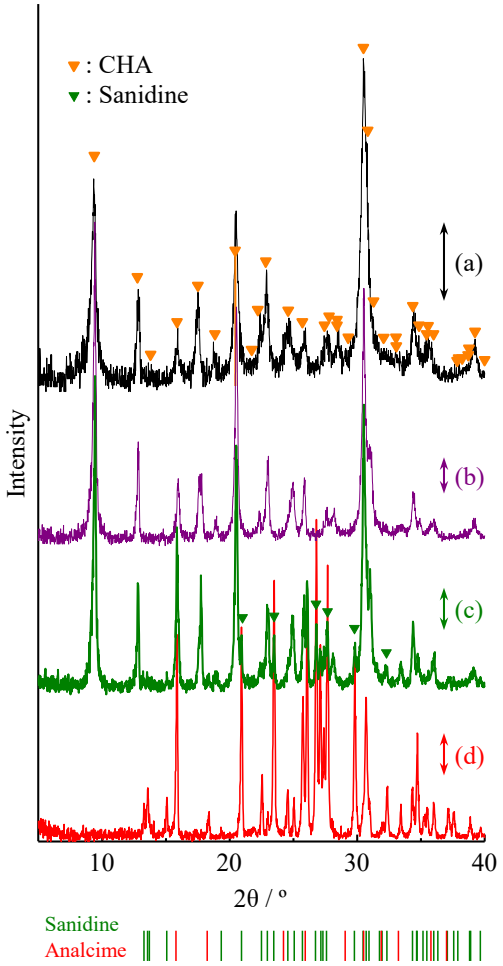

Fig. 1 XRD patterns of (a) CHA-HT, (b) CHA-Seed1, (c) CHA-Seed2 and (d) CHA-Seed3. The lengths of the arrows beside (a) to (d) each correspond to 100 cps. The expected positions of signals from sanidine and analcime are schematically drawn at the bottom.

Using CHA-HT as seed crystals, the growth of CHA zeolite with an amorphous aluminosilicate gel under hydrothermal conditions was investigated. Here, the mixed solution of fumed silica (1.0 g, Cab-O-Sil (M-5); Cabot Corporation, USA), $NaAlO_2$ (0.13 g), NaOH (0.47 g), KOH (0.17 g; all from Wako Pure Chemical Industries, Ltd.) in H_2O (30 mL) was used for preparing synthetic aluminosilicate gel according to the literature [14]. The molar

Table 1　Preparation and Si/Al ratio estimated by EDS and ^{29}Si MAS NMR measurements

Sample name	Synthetic conditions	Yield /g	Si/Al ratio	
			EDS	NMR
CHA-HT	Hydrothermally synthesized	-	2.5	2.17
CHA-Seed1	Synthesized using CHA-HT as a seed	0.45	3.0	2.73
CHA-Seed2	Synthesized using CHA-Seed1 as a seed	0.47	3.4	2.76
CHA-Seed3	Synthesized using CHA-Seed2 as a seed	0.41	4.0	n.d.

composition of this synthetic aluminosilicate gel corresponded to 1.0 SiO_2 : 0.1 $NaAlO_2$: 0.7 NaOH : 0.18 KOH : 100 H_2O. To this synthetic solution, CHA-HT (20 wt%, corresponding to about 0.36 g) as the seed crystals was added, and the mixture was hydrothermally treated at 170 ºC for 24 h with tumbling at 20 rpm using a hydrothermal synthesis reactor instrument (HIRO COMPANY). The product, denoted as CHA-Seed1 (see Table 1 for a summary of sample names), was obtained by filtration, drying and calcination in the same manner as mentioned above. The yield of CHA-Seed1 was higher than the weight of the seed crystals used, indicating that crystal growth from the synthetic alminosilicate gel had occurred.

The XRD pattern of CHA-Seed1 was as shown in Figure 1 (b). The diffraction signals were assignable to those from the CHA structure. Also, the diffraction signals were sharper and considerably more intense as compared with CHA-HT, suggesting that the crystallinity of CHA zeolite had been improved. The crystalline morphology of CHA-Seed1 observed by FE-SEM (JEM-6701F, JEOL) is represented in Figure 2 (b), together with that of CHA-HT (Figure 2 (a)). CHA-HT was composed from an aggregation of cube shaped crystals, the size of which generally ranging from several ten to 100 nm. On the other hand, CHA-Seed1 comprised of a stack of slab shaped crystals. The size of slabs was not uniform, ranging from several ten to several hundred nm. These were significantly different from those of CHA-HT, and the large sizes of crystals were consistent with the intense diffraction signals from CHA-Seed1.

In this study, further growth of CHA zeolites was also studied. CHA-Seed2 was prepared from the synthetic aluminosilicate gel in the same manner as mentioned above. Here, 20 wt% of CHA-Seed1 was used as seed crystals (Table 1). Subsequently, the resulting CHA-Seed2

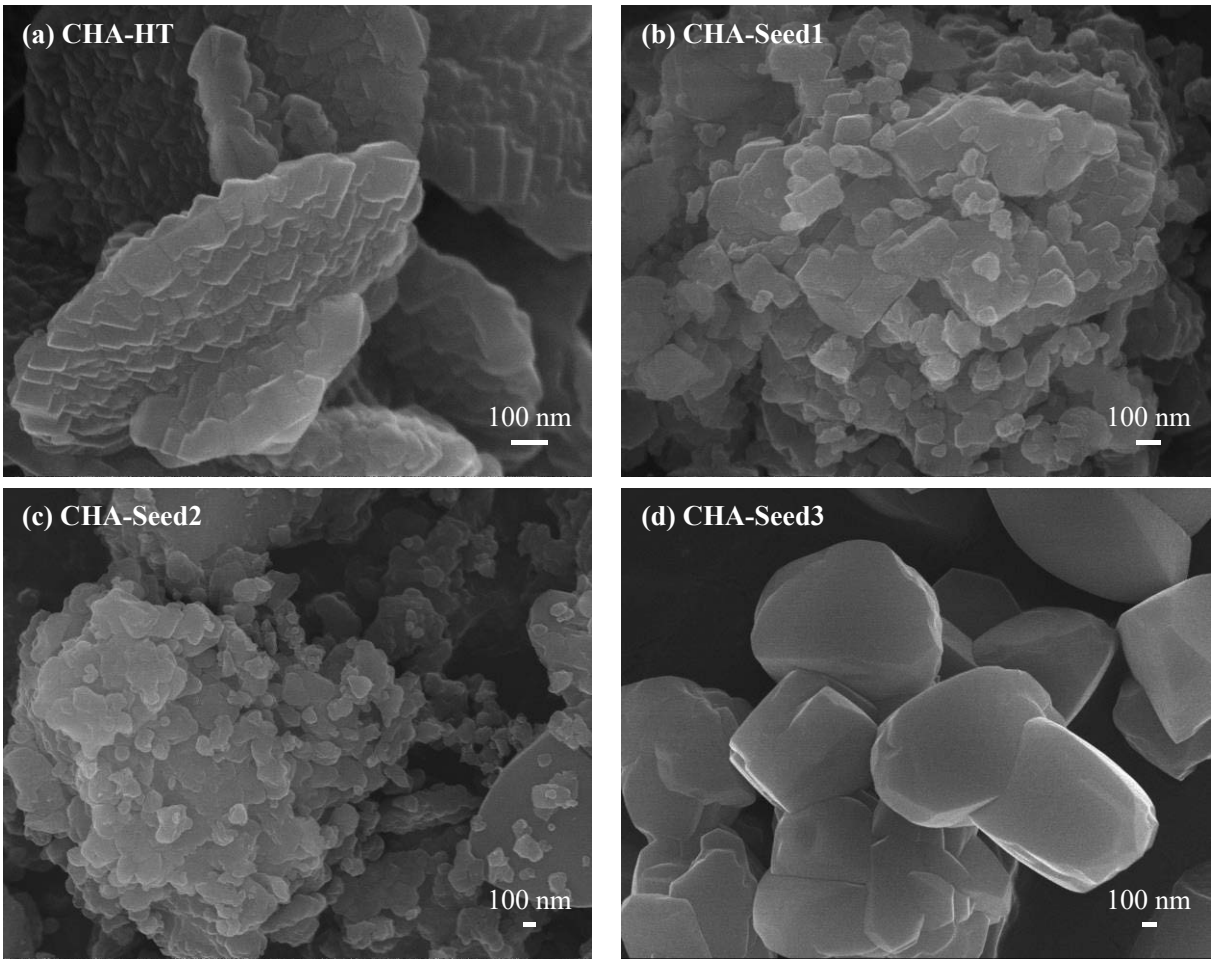

Fig. 2 FE-SEM pictures of (a) CHA-HT, (b) CHA-Seed1, (c) CHA-Seed2 and (d) CHA-Seed3.

was used as seed crystals for the preparation of CHA-Seed3. The XRD patterns of the obtained CHA-Seed2 and CHA-Seed3 were as shown in Figure 1. For the CHA-Seed2, although well-resolved and intense diffraction signals from the CHA structure could be confirmed, the diffraction signals assignable to sanidine (general formula; $(K,Na)(Si,Al)_4O_8$, JCPDS: 025-0618), for example, at 20.9, 23.5, 26.8, 27.7, 29.8 and 32.2º (2θ) were observed (marked signals in Figure 1 (c)). The latter signals, as well as other signals that appeared newly or had been hidden in the signals from CHA-Seed2, dominated in CHA-Seed3 (Figure 1 (d)). The diffraction signals were assignable to sanidine and analcime (ANA, general formula; $Na(Si_2Al)O_6 \cdot H_2O$, JCPDS: 041-1478) based on their peak positions illustrated in Figure 1. The drastic change of crystalline structure in CHA-Seed3 could be confirmed by FE-SEM study.

The crystalline morphology of CHA-Seed3, an aggregation of nonuniform ellipsoid-shaped crystals with the size of about several hundred to 1,000 nm, was totally different from that of CHA-HT or CHA-Seed1 (Figure 2). Thus, it was found that the seeded growth of CHA zeolite under hydrothermal conditions caused the collapse of specific CHA structures. Actually, the FE-SEM study of CHA-Seed2 showed large ellipsoid-shaped crystals rarely (e.g. on the right side in Figure 2 (c)), while the main product was slab shaped crystals.

The Si/Al ratio estimated by EDS (Energy-dispersive) spectroscopy (JEOL, JED-2300) combined with FE-SEM increased from 2.48 in CHA-HT to 2.97, 3.44 and 3.96 in CHA-Seed1, CHA-Seed2 and CHA-Seed3, respectively, showing an increase in Si content by the subsequence growth of CHA zeolite (Table 1). Imai et al. reported that the seed crystals mostly dissolved in this synthetic aliminosilicate gel in 1 h (170 ºC) [14]. Thus, the above results are consistent with the dissolution-recrystallization growth of CHA zeolite. Also, zeolites are not in a thermodynamically stable phase but in a metastable phase [16]. Therefore, the non-optimal synthetic conditions in this study is considered to have resulted in the formation of undesired aluminosilicates from CHA zeolite during repeated synthesis. It should be noted that the hydrothermal synthesis of aluminosilicate gel without seed crystals resulted in the formation of PHI type zeolite [2,14].

The growth and the structural change of CHA zeolite were investigated by using MAS (magic-angle spinning) NMR spectroscopy (at 6 kHz spinning, ECX-500, JEOL). Figure 3 shows the single-pulse spectra of ^{29}Si MAS NMR. Mainly, the resonance signals were observed at about -88, -92, -98, -103 and -108 ppm. These signals were assignable to Si(4Al), Si(3Al), Si(2Al), Si(1Al) and Si(0Al), respectively. Here, *n* in Si(*n*Al) indicates the number of Al atoms bonding to Si *via* O. One interesting point is that the relative intensities of Si(0Al) and Si(1Al) of CHA-Seed1 increased in comparison with those of CHA-HT. In addition, the

relative intensities of Si(3Al) and Si(4Al) decreased in CHA-Seed1. This suggests an increase in the number of Si-O-Si bonds in CHA zeolite made by seeded growth. CHA-Seed3, on the other hand, showed broadening of signals. As the XRD measurement revealed, CHA-Seed3 was a mixture of sanidine and analcime. Thus, the overlapping of Si(2Al) signals from two different aluminosilicates gave rise to the broadening of signals. Besides, sanidine is a polymorph crystal. This suggests that the heterogeneity of the Si tetrahedral environment led to the broadening of resonance signals.

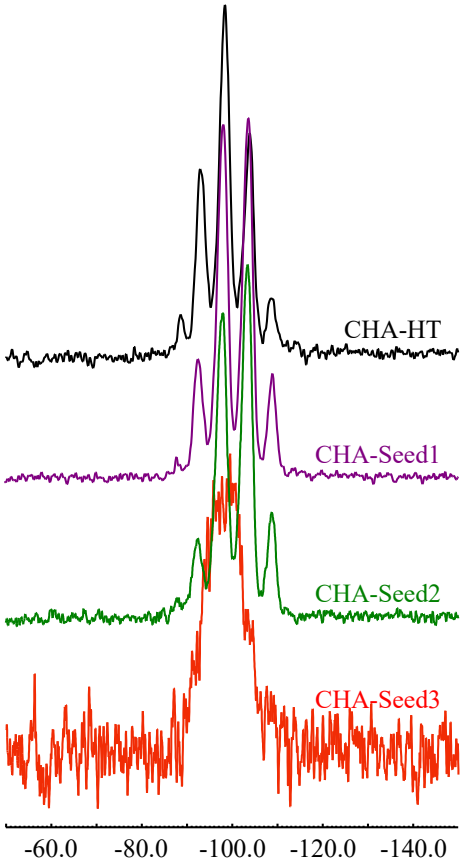

Fig. 3 ^{29}Si MAS NMR spectra of (a) CHA-HT, (b) CHA-Seed1, (c) CHA-Seed2 and (d) CHA-Seed3.

The framework Si/Al ratio can be determined from signal intensities using the following equation [17]:

$$(\mathrm{Si/Al}) = \sum_{n=0}^{4} A_{\mathrm{Si}\,(n\,\mathrm{Al})} \Big/ \sum_{n=0}^{4} \frac{n}{4} A_{\mathrm{Si}\,(n\,\mathrm{Al})}$$

Here, A is the signal area of Si(nAl). The Si/Al ratio was estimated to be 2.17, 2.73 and 2.76 for CHA-HT, CHA-Seed1 and CHA-Seed2, respectively (Table 1). An increase in the Si/Al ratio from CHA-HT to CHA-Seed1 was clearly observed, corresponding to the increase in signal intensity of Si(0Al) and Si(1Al). Also, it was found that these values were close to the ones obtained by EDS study (Table 1). However, a large difference was found between the Si/Al ratios determined by EDS and MAS NMR for CHA-Seed2, due to the presence of sanidine as evidenced by XRD.

Figure 4 shows the ^{27}Al MAS NMR spectra of CHA zeolites. The chemical shift of tetrahedrally coordinated Al atoms was found at 58.1, 58.6, 58.6 and 59.1 ppm for CHA-HT, CHA-Seed1, CHA-Seed2 and CHA-Seed3, respectively. The absence of the signals from octahedrally coordinated Al (around 0 ppm) suggests that Al atoms exist in the zeolite framework. The signal width became wider in CHA-Seed3 (9.108 ppm) as compared with CHA-HT (4.060), CHA-Seed1 (3.992) and CHA-Seed2 (4.449). Such broadening of resonance signals in CHA-Seed3 was consistent with the results of the ^{29}Si MAS NMR study.

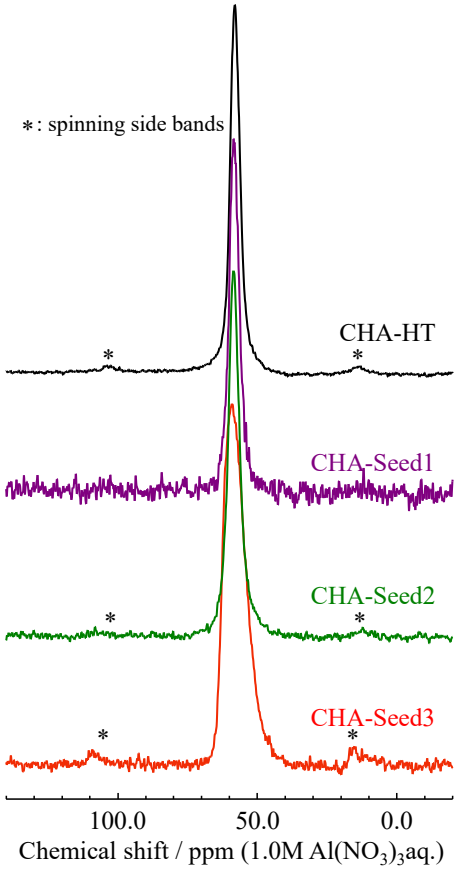

Fig. 4 ^{27}Al MAS NMR spectra of (a) CHA-HT, (b) CHA-Seed1, (c) CHA-Seed2 and (d) CHA-Seed3.

Finally, the N_2 adsorption isotherm of CHA zeolites at 77 K (Autosorb-1MP, Quantachrome Instruments, USA) were shown in Figure 5. The N_2 adsorption isotherm of CHA-HT did not indicate the occurrence of micropore filling (P/P_0 below 0.1), but showed a linear increase in N_2 adsorption up to about 0.8 (P/P_0) [13], suggesting the hindered access of N_2 molecules to micropores due to the presence of relatively large potassium cations (K^+). The K/Al ratio estimated by EDS was 1.1, 0.7 and 0.6 for CHA-HT, CHA-Seed1 and CHA-Seed2, respectively,

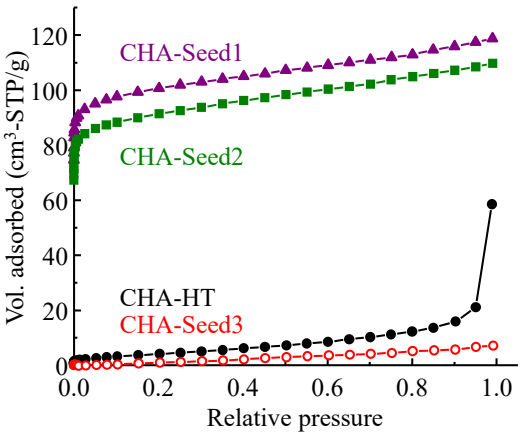

Fig. 5 Nitrogen adsorption isotherm of (a) CHA-HT, (b) CHA-Seed1, (c) CHA-Seed2 and (d) CHA-Seed3.

suggesting K^+ ions were filled almost fully in the cages of CHA-HT. As expected, CHA-Seed1 and CHA-Seed2 with lower K/Al ratios showed obvious micropore filling (type I by IUPAC classification) [18]. The N_2 sorption amount of CHA-Seed2 was slightly smaller than that of CHA-Seed1. This is due to the presence of non-porous sanidine in CHA-Seed2. For the mixture of sanidine and analcime (CHA-Seed3), the N_2 sorption amount was low in the whole (P/P_0) region. The BET (Brunauer-Emmett-Teller) surface area for CHA-HT, CHA-Seed1 and CHA-Seed2 was estimated to 14.0, 389.2 and 344.0 m^2/g, respectively. The surface area of CHA-Seed3 was lower than the value for detection limit (below 10 m^2/g).

In conclusion, CHA type zeolite was synthesized by seeded growth method, where OSDA-free CHA zeolite was used as seed crystals. The XRD measurements and ^{29}Si and ^{27}Al MAS NMR studies revealed that the obtained CHA zeolite were highly crystalized as compared with the initial material. However, the subsequent use of resultant CHA zeolite as seed crystals was found to be inappropriate, since other aluminosilicates – sanidine and analcime – were formed, resulting in a structure change.

References

[1] E. T. C. Vogt, G. T. Whiting, A. Dutta Chowdhury, B. M. Weckhuysen, Adv. Catal. 58 (2015) 143.
[2] http://www.iza-structure.org/databases/
[3] N. Nishiyama, M. Kawaguchi, Y. Hirota, D. Van Vu, Y. Egashira, K. Ueyama, Appl. Catal. A. Gen. 362 (2009) 193.
[4] X. Zhu, J. P. Hofmann, B. Mezari, N. Kosinov, L. Wu, Q. Qian, B. M. Weckhuysen, S. Asahina, JH. Ruz-Martínez, E. J. M. Hensen, ACS Catal. 6 (2016) 2163.
[5] Y. Ji, M. A. Deimund, Y. Bhawe and M. E. Davis, ACS Catal. 5 (2015) 4456.
[6] F. Gao, J. H. Kwak, J. Szanyi, C. H. F. Peden, Top. Catal. 56 (2013) 1441.
[7] R. Zhang, N. Liu, Z. Lei, B. Chen, Chem. Rev. 116 (2016) 3658.
[8] S. Vishnu Priya, T. Ohnishi, Y. Shimada, Y. Kubota, T. Masuda, Y. Nakasaka, M. Matsukata, K. Itabashi, T. Okubo, T. Sano, N. Tsunoji, T. Yokoi, M. Ogura, Bull. Chem. Soc. Jpn. 91 (2018) 355.
[9] S. I Zones, U.S. Patent 4,544,538, Oct. 1 (1985).
[10] S. I. Zones, J. Chem. Soc. Faraday Trans. 87 (1991) 3709.

[11] M. Bourgogne, J. L. Guth and R. Wey, U.S. Patent 4,503,024, March 5, 1985.
[12] M. Itakura, I. Goto, A. Takahashi, T. Fujitani, Y. Ide, M. Sadakane, T. Sano, Micropor. Mesopor. Mater. 144 (2011) 91.
[13] A. Taguchi, T. Nakamori, Y. Yoneyama, International Symposium on Zeolites and Microporous Crystals (ZMPC) 2018, Yokohama, submitted.
[14] H. Imai, N. Hayashida, T. Yokoi, T. Tatsumi, Micropor. Mesopor. Mater. 196 (2014) 341.
[15] Z. Liu, T. Wakihara, K. Oshima, D. Nishioka, Y. Hotta, S. P. Elangovan, Y. Yanaba, T. Yoshikawa, W. Chaikittisilp, T. Matsuo, T. Takewaki, T. Okubo, Angew. Chem. Int. Ed. 54 (2015) 5683.
[16] C. S. Cundy, P. A. Cox, Micropor. Mesopor. Mater. 82 (2005) 1.
[17] J. Klinowski, S. Ramdas, J. M. Thomas, C. A. Fyfe, J. S. Hartman, J. Chem. Soc. Faraday Trans. II, 78 (1982) 1025.
[18] M. Thommes, K. Kaneko, A. V. Neimark, J. P. Olivier, F. Rodriguez-Reinoso, J. Rouquerol, K. S. W. Sing, Pure Appl. Chem. 87 (2015) 1051.